HHS Public Access

Author manuscript

Mol Neurobiol. Author manuscript; available in PMC 2022 October 01.

Published in final edited form as:

Mol Neurobiol. 2021 October ; 58(10): 4787–4801. doi:10.1007/s12035-021-02461-3.

Glutamate Delta-1 Receptor Regulates Inhibitory Neurotransmission in the Nucleus Accumbens Core and Anxiety-Like Behaviors

Dinesh Y. Gawande[#1], **Gajanan P. Shelkar**[#1], **Jinxu Liu**[#1], **Anna D. Ayala**[1], **Ratnamala Pavuluri**[1], **Diane Choi**[2,3], **Yoland Smith**[2,3,4], **Shashank M. Dravid**[1,*]

[1]Department of Pharmacology and Neuroscience, Creighton University, 2500 California Plaza, Omaha, NE, USA

[2]Yerkes National Primate Research Center, Atlanta, GA 30329, USA

[3]UDALL Center of Excellence for Parkinson's Disease, Atlanta, GA 30329, USA

[4]Department of Neurology, Emory University, Atlanta, GA 30329, USA

[#] These authors contributed equally to this work.

Abstract

Glutamate delta-1 receptor (GluD1) is a member of the ionotropic glutamate receptor family expressed at excitatory synapses and functions as a synaptogenic protein by interacting with presynaptic neurexin. We have previously shown that GluD1 plays a role in the maintenance of excitatory synapses in a region-specific manner. Loss of GluD1 leads to reduced excitatory neurotransmission in medium spiny neurons (MSNs) in the dorsal striatum, but not in the ventral striatum (both core and shell of the nucleus accumbens (NAc)). Here, we found that GluD1 loss leads to reduced inhibitory neurotransmission in MSNs of the NAc core as evidenced by a reduction in the miniature inhibitory postsynaptic current frequency and amplitude. Presynaptic effect of GluD1 loss was further supported by an increase in paired pulse ratio of evoked inhibitory responses indicating reduced release probability. Furthermore, analysis of GAD67 puncta indicated a reduction in the number of putative inhibitory terminals. The changes in mIPSC were independent of cannabinoid or dopamine signaling. A role of feed-forward inhibition was tested by selective ablation of GluD1 from PV neurons which produced modest reduction in mIPSCs. Behaviorally, local ablation of GluD1 from NAc led to hypolocomotion and affected

[*]Corresponding author: ShashankDravid@creighton.edu.

Author contribution

DYG, GPS, JL, AA, RP, DC, YS, SMD conducted experiments, contributed to writing the manuscript and/or analyzed data. All authors contributed to research design and reviewed the final manuscript.

Conflict of interest

The authors declare no competing interests.

Code availability

Not applicable

Compliance with ethical standard

Ethics approval and consent to participate

All animal studies were approved by Creighton University, Institutional Animal Care and Use Committee.

Consent for publication

Not applicable

anxiety- and depression-like behaviors. When GluD1 was ablated from the dorsal striatum, several behavioral phenotypes were altered in opposite manner compared to GluD1 ablation from NAc. Our findings demonstrate that GluD1 regulates inhibitory neurotransmission in the NAc by a combination of pre- and postsynaptic mechanisms which is critical for motor control and behaviors relevant to neuropsychiatric disorders.

Keywords

Nucleus accumbens; GluD1; GRID1; Cbln1; Inhibition

Introduction

Ionotropic glutamate receptors are grouped into four families NMDA, AMPA, kainate, and delta receptors. The delta receptors are unique in that they do not exhibit typical ion channel currents, but instead function as synaptogenic molecules by interacting with presynaptic neurexin [1]. This interaction is mediated by Cbln1 and other Cblns released from presynaptic terminals. We have previously found that the loss of GluD1 reduces excitatory neurotransmission in specific brain regions. For example, in dorsal striatum medium spiny neurons (MSNs), the loss of GluD1 reduces mEPSC frequency. However, GluD1 deletion (GluD1 knockout) does not reduce excitatory neurotransmission in the cortex, hippocampus, and nucleus accumbens (NAc) shell and core [2–4]. Instead, excitatory neurotransmission and makers of excitatory synapses are upregulated in cortical and hippocampal regions in GluD1 knockout mice [2]. There are, however, studies using other strategies for GluD1 knockdown with sparse ablation that demonstrate that GluD1 is obligatory for the maintenance of excitatory synapses in the cortex and hippocampus [5]. Thus, the precise role of GluD1 in the regulation of excitatory neurotransmission in these regions and/or cell types remains to be further examined using a more comprehensive approach. In contrast, to the important role of GluD1 in excitatory neurotransmission in several regions, its relevance to inhibitory neurotransmission remains less understood. GluD1 has been found to be expressed in interneurons [6], and therefore if GluD1 is critical for excitatory inputs onto GABAergic interneurons, it may affect feed-forward inhibition. Alternatively, GluD1 was recently found to be important for the formation and maintenance of inhibitory synapses on pyramidal neurons in the somatosensory cortex [7]. It was found that GluD1-Cbln4 synaptogenic signaling is critical for the formation and maintenance of somatostatin interneuron mediated inhibitory synapses onto dendrites of pyramidal neurons. Interestingly, reporter model analysis has identified enriched expression of Cbln4 in several other nuclei including NAc [8]. Here, we investigated whether GluD1 regulates inhibitory neurotransmission in the NAc and its effect on motor function and behaviors relevant to neuropsychiatric disorders.

Our findings demonstrate that GluD1 loss reduced inhibitory neurotransmission in MSNs of the NAc core, in part through presynaptic mechanisms, where GluD1 does not affect excitatory neurotransmission [4]. Selective ablation of GluD1 from parvalbumin (PV)-positive GABAergic interneurons modestly reduced inhibitory neurotransmission in MSNs, potentially suggesting roles for GluD1 in additional interneurons in feed-forward inhibition.

In addition, we found a decrease in the density of GAD67 puncta in the NAc core, suggesting a reduction in the prevalence of inhibitory GABAergic synapses in NAc core upon GluD1 ablation. Finally, local ablation of GluD1 from the NAc produced effects on locomotor and anxiety-like behaviors which were partly reproduced by specific GluD1 deletion from striatal PV interneurons. These results suggest that GluD1 is obligatory for normal inhibitory neurotransmission in the NAc, and that this effect is mediated by a combination of feed-forward inhibition and direct effects on inhibitory synapses.

Methods

Animals

Wildtype and GluD1 KO mice [9] were used for these studies. Mice were group housed at a constant temperature (22 ± 1 °C) and a 12-h light-dark cycle with free access to food and water as previously described [10]. GluD1$^{flox/flox}$ mice were a kind gift from Dr. Pei Lung-Chen with loxP sites in intron 10 and 12. The GluD1$^{flox/flox}$ mice were crossed with PV-cre mice from Jax (Catalog number 017320) to selectively ablated GluD1 from PV interneurons. In this study, strict measures were taken to minimize pain and suffering to animals in accordance with the recommendations in the Guide for Care and Use of Laboratory Animals of the National Institutes of Health. All experimental protocols were approved by the Creighton University Institutional Animal Care and Use Committee Policies and Procedures.

Electrophysiology

Whole-cell electrophysiology was performed as previously described [2,11]. After isoflurane anesthesia, mice (P28–35) were decapitated and brains were removed rapidly and placed in ice-cold artificial cerebrospinal fluid (ACSF) and sectioned into 300-μm thick parasagittal sections. The ACSF composition was as follows (in mM): 130 NaCl, 24 $NaHCO_3$, 3.5 KCl, 1.25 NaH_2PO_4, 0.5 $CaCl_2$, 3 $MgCl_2$ and 10 glucose saturated with 95% O_2/5% CO_2. Whole-cell patch recordings were obtained from MSNs in voltage-clamp configuration using Axopatch 200B. Signal was filtered at 2 kHz and digitized at 10 kHz using an Axon Digidata 1440A analog-to-digital board (Molecular Devices, CA, USA). Glass pipette with a resistance of 5–8 mOhm were filled with an internal solution consisting of (in mM) 110 cesium gluconate, 30 CsCl, 5 HEPES, 4 NaCl, 0.5 $CaCl_2$, 2 $MgCl_2$, 5 BAPTA, 2 Na_2ATP, and 0.3 Na_2GTP (pH 7.35). QX314 was added to block voltage-gated sodium channels. Whole-cell recordings with a pipette access resistance less than 20 mOhm and that changed less than 20% during the duration of recording were included. IPSCs were evoked by a bipolar tungsten electrode (World Precision Instruments, FL, USA) placed at the border between NAc core and the cortex dorsal to the anterior commissure. Neurons were held at a holding potential of 0 mV for mIPSCs. For recording mIPSCs 0.5 μM tetrodotoxin, 10 μM CNQX and 100 μM DL-AP5 were added to the external recording solution. The mIPSC recordings were analyzed using Minianalysis software (Synaposoft, Atlanta, GA, USA) with an amplitude threshold set at 5 pA. Frequency, amplitude and decay of the miniature currents were determined.

Immunohistochemistry

Immunohistochemistry was performed as previously described [2–4,11]. Briefly, mice were transcardially perfused with 4% PFA, brains collected and post-fixed and processed for cryopreservation. Thereafter, 25-μm thick sagittal or coronal sections passing through NAc core were obtained and processed for immunolabeling. Sections were washed in 0.1M PB (prepared by adding 0.1 M NaH_2PO_4 (2.3996 g in 200 ml of ddH2O) to 0.1M Na_2HPO_4, (10.64 g in 750 ml of ddH_2O) till pH is 7.4), before incubation in a blocking solution containing 10% normal goat serum or normal donkey serum in 0.25% Triton-X in 0.1 M PB (PBT) for 1 h at room temperature. Sections were then incubated overnight at 4 °C in the single or combination of following primary antibodies: guinea pig anti-GluD1 (1:500, GluD1C-GP-Af860, Frontier Institute Co., Ltd, Japan), rabbit anti-PV (1:500, Swant PV27) rabbit anti-somatostatin (1:500, T4103, BMA Biomedical Peninsula Labs), rabbit anti-vGluT1 (1:5000, Mab Tech, VGT1–3), chicken anti-vGluT2 (1:300, Synaptic System, 135416), mouse anti-GAD 67 (1:500, Millipore, MA, USA). On the next day, sections were washed with 0.1 M PB (6 times for 5 min each) and incubated with single or combination of appropriate secondary antibodies, goat anti-guinea pig antibody conjugated to AlexaFluor 488 (1:500, A11073, Thermo Fisher Scientific), goat anti-mouse antibody conjugated to AlexaFluor 594 (1:500, A11005, Thermo Fisher Scientific), and goat anti-rabbit antibody conjugated to AlexaFluor 594 (1:500, A11012, Thermo Fisher Scientific), goat anti-chicken antibody conjugated to AlexaFluor 594 (1:500, A11042, Thermo Fisher Scientific), for 2 h at room temperature in dark. Sections were washed with 0.1 M PB (3 times for 5 min each), mounted and coverslipped with Fluoromount-G. Images were acquired with an Infinity camera (Lumenera Co., Ottawa, ON, Canada) coupled to a fluorescence microscope (Nikon Eclipse Ci, Melville, NY, USA) using the Lumenera Infinity Analyze software (Lumenera Co.) or with Nikon Ti-E inverted microscope with a Yokagawa spinning disc for confocal imaging scanning confocal microscope. For puncta analysis, images of equivalent regions, 1024 × 1024 pixels, were captured using a 60×, oil-immersion objective at a 1× zoom. The NAc core was scanned at 0.3 μm intervals along the z-axis and an optical section (7.2 μm thick) was taken from each tissue section. Co-localization and the puncta number were analyzed by Volocity (PerkinElmer Inc. Coventry, UK). Briefly, libraries were created from raw data files generated during image acquisition. The analysis algorithm sequence was setup from list of existing protocols in Volocity to identify different objects (puncta) imaged in separate channels (detectors) and their colocalization. Selection of the relevant objects was optimized based on fluorescence intensity and categorizing objects by size range. The individual files were then processed for object (puncta) identification and colocalization analyses. The detection of fluorescence signals from separate channels in the same voxel was considered as colocalization. Automatically calculated numeric values by software for individual puncta and colocalization were collated and plotted for comparisons.

Electron microscopy

The brains of three mice were EM immunostained with a highly specific GluD1 antibody [12] using the immunoperoxidase and pre-embedding immunogold methods, as described in our previous studies [13,14]. The immunoperoxidase-stained tissue was used to determine the overall pattern of neuronal and glial GluD1 labeling, while the immunogold-labeled material was used to assess the subsynaptic localization of GluD1. In the electron

microscope, random series of 50 micrographs of GluD1-immunoreactive profiles were taken at 25,000× from the surface of blocks of NAc tissue immunostained with peroxidase. From these images, GluD1-immunoreactive elements were categorized as dendrite, spine, axon/terminal or glial profiles based on their well ultrastructural features [15]. These elements were counted and expressed as relative percentage of total labeled elements in the NAc core. In the case of the immunogold-stained tissue, ultrathin sections were screened for the presence of synaptic (ie in the main body of the post-synaptic density) or peri-synaptic (i.e. at the edges of the post-synaptic density) GluD1 labeling. When such labeled elements were found, they were photographed at 25,000× and 60,000× so that the type of synapses and the morphology of the pre- and post-synaptic structures could be further studied.

Stereotaxic surgery and viral delivery

Stereotaxic surgery and viral delivery were performed as previously described [3]. Mice were anesthetized with isoflurane and placed in a stereotaxic frame. The skull was exposed, and small hole was drilled through the skull at the coordinates for dorsal striatum (AP: +0.9 mm, ML: ±1.5 mm, DV: −3 mm) or ventral striatum (AP: +1.6 mm, ML: ±0.8 mm, DV: −4.2 mm). All the coordinates were taken with respect to the bregma. The virus particles AAV9.hsyn.eGFP/AAV9.hsyn.eGFP-Cre (University of Pennsylvania vector core) suspended in phosphate buffered saline were injected by using microliter syringe (NanoFil, World Precision Instruments, Sarasota, FL, USA) with 33-gauge beveled needle (NF33BV-2, World Precision Instruments). The injection needle was lowered, and virus particles were delivered at a rate of 1nl/sec using a UMP3 micro-syringe pump (World Precision Instruments). The volume of injections was kept at 150 nl to obtain the precise local infection and to avoid the leak into other brain regions. The needle was left in place for additional 10 min at the injection site and was slowly withdrawn over the period of 5 min. The incision was sealed with surgical tissue adhesive (1469SB, 3M, Maplewood, MN, USA). Postoperatively, local analgesic and triple antibiotic was applied externally onto the surgery site and mice were monitored on a heat pad for one hour before being returned to their home cage. Mice received postoperative care for at least 3 days after surgery. Analysis of the brain tissue after completion of behavioral experiments demonstrated localization of AAV injections and downregulation of GluD1 in cre group similar to our previous studies using this methodology [3]. In addition, similar to our previous observations [3], injections in ventral striatum were found to preferentially localize to the core region compared to shell region of the nucleus accumbens.

Behavior

Open field test—Open field test was performed in a custom-made square box (38 cm × 38 cm × 30 cm). Each animal was placed in the open field chamber and the behavior was videotaped. Total distance travelled in the box was scored using AnyMaze video-tracking software (Stoelting, Wood Dale, IL, USA).

Zero maze test—For zero maze test testing, mice were introduced into a custom-made circular elevated maze (50-cm diameter, 5-cm track width,) with 50% enclosed (12-cm wall height) and 50% open arenas. Mice were allowed to freely explore the novel environment for

5 min. All sessions videotaped and duration and entries into open arm were recorded with the experimenter blind to the genotype.

Spontaneous Y-maze alternation test—Mice were place in the Y-maze and spontaneous alternations were recorded for 8 min. Mice which did not show any new entries for a period of more than 2 min during the test were excluded from the study. Alternation was defined as consecutive entries into each of the arms without repetition. Percent spontaneous alternation was calculated as number of actual alternations divided by possible alternations (i.e. total arm entries-2) × 100.

Novel object recognition test—Recognition memory was assessed to determine potential short-term and long-term memory deficits. The novel object recognition chamber was a square open field (25.4 × 25.4 × 17.8 cm). The novel object recognition task was performed in three phases; environmental acclimation, training and testing. During acclimation all animals were handled 1–2 min a day for 3 days. On days 2 and 3 of handling, animals were placed in the experimental apparatus for 10 minutes to acclimate animals to the environment. On days 4 and 5 of training mice were placed in the chamber with two identical objects and allowed to explore for 10 min. Sixty minutes after training on day 5 short-term memory was assessed (T1) by exchanging one familiar object with a novel object. Mice were allowed to explore the experimental apparatus for 10 min. Time spent inspecting both the novel and familiar objects within a 3-cm radius were recorded. Location of the novel object was counterbalanced with half of animals in each group exposed to the novel object on the left side of the chamber and the other half exposed on the right side of the chamber. A second (T2) novel object was presented 24 h after training to test for long-term memory, again location of the novel object was counterbalanced in the chamber. All objects were cleaned with 70% ethanol between trials to eliminate potential olfactory cues or preference for each object.

Marble burying test—Marble burying test was conducted in a 25×25-cm arena with the home cage bedding to a height of 5 cm. White light of 300–330 lux intensity was used to evenly illuminate the entire arena of the marble burying test. 36 dark colored marbles 1.5 cm in diameter were placed 5 cm apart. The test mouse was placed in the same corner of the open field arena and left in the arena for 30 min. At the end of the 30 min the mouse was taken out and the number of marbles buried was counted. If two-thirds of a marble was buried inside the bedding it was counted as buried otherwise non-buried.

Social interaction test—Social interaction test was performed as described previously [16] with slight modifications. The sociability test apparatus comprised of a rectangular, three chambered plexiglass box. Each of the three chambers was 20-cm length × 40.5-cm width × 22-cm high. The dividing walls were made of clear plexiglass. The small doorways at center of each dividing wall allowed the access to each chamber. During the acclimatization, each chamber was isolated by using dividing walls. Clear plexiglass cylindrical containers with holes were placed in center of right and left chamber. On one side, an unfamiliar (animate) mouse was enclosed in the cylindrical container and while the container on the other side was left empty (referred to as inanimate object). Subsequently,

the experimental mouse was placed in the middle chamber and allowed to acclimatize for 5 min. Thereafter, the doors on either side were opened and the experimental mouse was allowed to explore animate and inanimate cylinders for 10 min. A circle 1 cm beyond the periphery of the plastic containers was marked. The time spent by the experimental mouse within this circle interacting with the inanimate- or animate-containing plastic container was recorded and reported.

Forced swim test—Forced swim test was conducted to assess depression-like behavior. The test was conducted in a glass cylinder measuring (30-cm height × 20-cm diameter). The cylinder was filled with water (23–25 °C) to ~15 cm of height. Each mouse was gently placed into the cylinder and swimming activity was videotaped for 6 min. The prerecorded videos were scored manually by the experimenter blind to the genotype and treatment. To avoid novelty-induced differences, the first 2 minutes of the test were excluded and the videos were scored for the remaining 4 minutes. Mobility was any movement other than those necessary to maintain balance and to keep head above water level.

Statistics

Data were analyzed using unpaired t-test, one-way ANOVA or two-way ANOVA with post-hoc multiple comparisons test. Differences were considered significant if $P < 0.05$. Prism 6 (GraphPad Software Inc., San Diego, CA, USA) was used for analysis and representation.

Results

GluD1 knockout have lower inhibitory neurotransmission in the nucleus accumbens MSNs

We analyzed mIPSC from core and shell regions of the NAc MSNs. In recordings from NAc core, we found that loss of GluD1 results in lower mIPSC amplitude and frequency ($P = 0.0028$ and $P = 0.0491$ for bar graph of mIPSC amplitude and frequency respectively, unpaired t-test; $P < 0.05$ for cumulative probability of mIPSC amplitude and frequency, K-S test; Fig. 1A), whereas no change in mIPSC amplitude and frequency were observed in NAc shell recordings (Fig. 1B), indicating that GluD1 has a region-specific effect on inhibitory neurotransmission.

No change in modulation of inhibitory neurotransmission by cannabinoid and dopamine signaling in GluD1 knockout

Dopamine released from ventral tegmental area (VTA) dopaminergic inputs has also been shown to regulate inhibitory synaptic transmission via dopamine D1 receptor in nucleus accumbens [17,18]. Moreover, Benamer et al. reported that GluD1 deletion decreased the burst firing of dopaminergic neurons in substantia nigra pars compacta (SNc) and VTA [19]. Thus, we evaluated whether changes in basal tone of the dopaminergic system underlied the differences in inhibitory neurotransmission seen in the NAc core of GluD1 KO mice. To test if GluD1 deletion affects dopamine tone in the NAc, we applied a dopamine D1 receptor antagonist SCH23390. We found that SCH23390 application produced a reduction in the amplitude and frequency of mIPSC. However, this effect was observed to a similar extent in wildtype and GluD1 KO mice, indicating no change of tonic dopaminergic tone on MSNs in GluD1 KO animals (Fig. 2A). Postsynaptically-released endocannabinoids regulate

GABA release by acting on presynaptic CB1 receptors in NAc [20,21]. In NAc core, we found no evidence for tonic endocannabinoid regulation of GABA release and changes in GluD1 KO, as bath application of a CB1 receptor inverse agonist (rimonabant) did not alter mIPSC amplitude and frequency in either genotype (Fig. 2B). Thus, differences in local dopamine and cannabinoid signaling may not account for the differences in basal inhibitory neurotransmission seen in GluD1 KO mice.

We next analyzed whether the plasticity of inhibitory synapses may be affected by loss of GluD1. Activation of presynaptic CB1 receptors induces depression of inhibitory synapses in the NAc. We evaluated the effect of CB1 receptor agonist (CP55940) on evoked IPSCs. A strong and similar reduction in the amplitude of evoked IPSC was observed in both wildtype and GluD1 KO mice (Fig. 2C), suggesting no effect of GluD1 loss on CB1-induced depression of inhibitory synapses. We further evaluate the paired pulse ratio. Interestingly, we detected an increase in paired-pulse ratio of evoked IPSCs in GluD1 KO ($P = 0.0066$, unpaired t-test; Fig. 2D) suggesting a lower probability of GABA release. To ensure that this effect was due to a change in release probability and not the recovery of synapses after the first pulse, we analyzed the amplitude of the first responses in wildtype and GluD1 KO. A significantly lower amplitude of first evoked IPSC was noted in the GluD1 KO (WT, 176.28 ± 10.20 pA versus GluD1 KO, 134.68 ± 14.09 pA, $N = 10–11$, $P = 0.0288$, unpaired t-test), suggesting a reduced release in the first stimulus and a change in the overall release probability.

GluD1 loss reduces number of inhibitory synapses in the NAc core

Recent studies have demonstrated a direct effect of GluD1 in the formation of inhibitory synapses by interacting with Cbln4 expressed in somatostatin-positive interneurons in the somatosensory cortex [7]. Because Cbln4 is enriched in NAc [8], it is possible that GluD1 has a direct effect on the formation of inhibitory synapses in the NAc. To test this hypothesis, we first examined whether GluD1 is localized to excitatory or inhibitory synapses. Using confocal microscopy double labeling immunohistochemical approaches, our studies showed that GluD1 co-localize with both excitatory (vGluT1 and vGluT2) and inhibitory (GAD67) markers of axon terminals (Fig. 3A). Next, we examined the abundance of GAD67 puncta in wildtype and GluD1 KO mice. We observed a significant reduction in total GAD67 puncta ($P < 0.0001$, Fig. 3B) suggesting that the total number of inhibitory synapses may also be reduced upon ablation of GluD1. Together, these results demonstrate that the reduced inhibition in MSNs may involve both direct effect on inhibitory synapses and reduced release probability from GABAergic terminals.

The expression of GluD1 at putative glutamatergic and GABAergic synapses was further confirmed at the electron microscopic level using the pre-embedding immunoperoxidase and immunogold methods in 3 wildtype mice. In the electron microscope, accumbens GluD1 immunoperoxidase staining was expressed in both neuronal and glial profiles. From the immunoperoxidase-stained tissue, analysis of a total of 513 GluD1-immunoreactive elements could be categorized on the basis of their ultrastructural features as follows, 20 +/− 5% were dendritic shafts, 15 +/− 6% were spines, 41 +/− 18% were pre-synaptic axonal or terminal profiles and 24 +/− 12% were glia (Fig. 3C,D). In the immunogold-stained

tissue, synaptic gold particles labeling was either peri-synaptic (or at the edges) to putative glutamatergic asymmetric axo-spinous or axo-dendritic synapses (Fig. 3 E,F) or in the main body of putative GABAergic symmetric synapses (Fig. 3G).

Modest effect of GluD1 deletion from PV neurons on inhibitory neurotransmission

GluD1 has been found to express in interneurons [6], and in the striatum RNAseq suggest GluD1 expression in PV, SOM and ChAT interneurons [22,23]. We examined the expression of GluD1 in these cell types using immunohistochemistry. Indeed, GluD1 puncta were localized to both dendrites and soma of PV- and SOM- cells (Fig. 4A, Supplementary Fig. 1A). It has recently been found that VTA glutamatergic neurons send excitatory projections to GABAergic neurons particularly PV-interneurons, in the NAc which then send feedforward inhibitory inputs onto MSNs [24]. In addition, Cbln1, the synaptogenic partner of GluD1, is expressed in the VTA [25]. Thus, it is possible that Cbln1-GluD1 complexes may lead to the formation of glutamatergic synapses on PV-interneurons, thereby indirectly affecting inhibitory tone onto MSNs. To test this hypothesis, we examined the effect of selective ablation of GluD1 from PV interneurons on inhibitory neurotransmission in the NAc. Conditional deletion of GluD1 was achieved using $GluD1^{flox/flox}$ and PV-Cre mouse line. No change in the total number of PV neurons was found upon GluD1 deletion (Fig. 4B). Electrophysiology studies revealed no significant change in the frequency of mIPSC recorded from MSNs in mice with deletion of GluD1 from PV interneurons, however a significant reduction in the amplitude of mIPSC was observed ($P = 0.0337$, Fig. 4C).

GluD1 deletion from NAc affects anxiety- and depression-like behavior

Finally, we examined the potential effect of regulation of inhibitory neurotransmission by GluD1 in the NAc on mouse behavior. We examined behaviors in mice with conditional ablation of GluD1 from the NAc. For these experiments, stereotaxic injection of AAV-control or AAV-Cre was conducted into the NAc of $GluD1^{flox/flox}$ mice and after sufficient time interval for Cre expression and GluD1 ablation behavioral battery was conducted. AAV expression and location and GluD1 ablation was confirmed at the end of experiment (Fig. 5J, 5K). We found that deletion of GluD1 from the NAc resulted in reduced locomotor activity ($P = 0.0423$, unpaired t-test; Fig. 5C). In the zero maze test, mice with AAV-Cre injection spent less time in open area suggesting higher anxiety-like behavior ($P = 0.0486$; Fig. 5D). In marble burying test, GluD1 deletion from NAc resulted in reduced marble burying behavior ($P = 0.0229$; Fig. 5F). Finally, AAV-Cre mice also exhibited more mobile events ($P = 0.0251$) and less immobile events ($P = 0.0373$) in the forced swim test compared to AAV-control (Fig. 5I). Thus, ablation of GluD1 from the ventral striatum produces changes in anxiety and depression-like behaviors.

Interestingly, the behaviors produced by ablation of GluD1 in the NAc core were opposite to those observed after GluD1 deletion in the dorsal striatum. Specifically, mice with ablation of GluD1 from the dorsal striatum displayed hyperlocomotion ($P = 0.0316$; Fig. 6C), spent more time in open area ($P = 0.0316$; Fig. 6D) and more frequently entered open area ($P = 0.0316$; Fig. 6D') in the zero maze but did not exhibit any change in depression-like behavior (Fig. 6I). Thus, ventral and dorsal striatal GluD1 contributes differentially to behavior.

We also assessed behavioral changes in mice with conditional deletion of GluD1 in PV-interneurons. These mice behavior partially mirrored that of mice with GluD1 deletion in NAc. Specifically, a significant reduction in marble burying (P = 0.0137) and increase in mobile events in the forced swim test (P = 0.0133) were observed (Fig. 7D, F, I). Interestingly, social interaction with stranger mouse was reduced in mice with GluD1 deletion from PV neurons (Fig. 7G). In addition, an increase in MK-801-induced hyperlocomotion, a model of psychosis, was observed in mice with deletion of GluD1 from PV neurons (Supplementary Fig. 2C, C'). Together, these changes in social behavior and MK-801-induced hyperlocomotion are relevant to schizophrenia-like phenotypes.

Discussion

GluD1 regulates inhibitory neurotransmission in the NAc by multiple mechanisms

The delta family of glutamate receptors are unusual in that they serve as synaptogenic molecules by partnering with presynaptic neurexin via intermediate proteins Cblns [26–28]. The role of GluD2 and GluD1 in excitatory neurotransmission has previously been identified [1–4]. More recently, GluD1 has also been found to play an important role at inhibitory synapses in the somatosensory cortex via interactions with Cbln4 [7]. We have previously found that GluD1 modulates properties of excitatory synapses in the NAc in basal state and upon cocaine exposure [4]. However, GluD1 deletion did not lead to an overall reduction in AMPA mEPSC frequency or amplitude suggesting that GluD1 is not obligatory for the formation of excitatory synapses. In the present study, we found that GluD1 loss affects inhibitory neurotransmission in the core, but not the shell, of NAc. We found a reduction in both the frequency and amplitude of mIPSC. In addition, we found an increase in PPR suggesting changes in release probability at inhibitory synapses. No change in cannabinoid or dopamine tone was observed in the GluD1 KO and plasticity of inhibitory synapses was also unaffected. We provide confocal and electron microscopy evidence that GluD1 is expressed at both excitatory and inhibitory synapses in the NAc core. Furthermore, a reduction in the relative abundance of GAD67 puncta suggest a significant decrease in the number of inhibitory synapses in the NAc core of GluD1 knockout. Overall, GluD1 was found to regulate inhibitory neurotransmission by multiple mechanisms.

Potential synaptogenic function of GluD1 for inhibitory synapses

It has previously been found that GluD1 may induce inhibitory synapse formation in cell culture model [29]. In addition, reduction in inhibitory synapse marker GAD67 has been found in the hippocampus of GluD1 knockout mice [30]. A recent study has found that GluD1 is responsible for the formation of inhibitory synapses in the somatosensory cortex [7]. GluD1 mediates its effects at excitatory synapses via its synaptogenic partner Cbln1. Instead, in the somatosensory cortex Cbln4 serves as a synaptogenic partner of GluD1 in the formation of inhibitory synapses [7]. Although, early studies suggested lack of Cbln4 in the NAc [31], recent studies using Cbln4 reporter model have found strong expression of Cbln4 in the somata of interneurons in the NAc [8]. Furthermore, RNAseq analysis also indicates expression of Cbln4 in interneurons particularly in PV-, SOM- and ChAT-positive neurons in the striatum [22,23]. Thus, it is likely that in the NAc, Cbln4 may interact with GluD1 and contribute to the formation of inhibitory synapses. Alternatively, it has also been

found that certain GABAergic neurons in the VTA also express Cbln1 [32] and if these neurons project to the NAc they may also contribute to the formation of inhibitory synapses together with GluD1. It is interesting to note that there is a lack of effect of GluD1 on the inhibitory neurotransmission in the dorsal striatum [3] even though Cbln4 is expressed in interneurons throughout the striatum [22,23]. Further studies are needed to address the precise presynaptic composition and input-specificity of the GluD1 mediated synaptogenic triad that may induce inhibitory synapses in a region-specific manner.

Contrasting role of GluD1 on neurotransmission and behavior in dorsal and ventral striatum

We have previously characterized opposite changes in behavioral flexibility and repetitive behavior in mice with ablation of GluD1 in the dorsal striatum versus ventral striatum [3]. Specifically, ablation of GluD1 from the dorsal striatum, but not ventral striatum affects behavioral flexibility in water T-maze test and leads to higher latency to fall in the rotarod test which is relevant to repetitive behavior. Here, our data further corroborates our earlier findings that GluD1 loss in dorsal or ventral striatum leads to opposite behavioral changes. One of the strongest phenotypes that was replicated in both models with deletion of GluD1 from dorsal or ventral striatum was a reduction in marble burying. In addition, this phenotype was replicated in PV-GluD1 KO mice. This phenotype has been associated with repetitive and anxiety-like behavior [33–35]. However, because ablation of GluD1 from dorsal and ventral striatum leads to opposing effects on locomotor activity and anxiety-like behavior in the zero maze, the specific phenotype in marble burying is likely to represent a combination of behavioral changes. We predict that the differential effect of GluD1 ablation from dorsal and ventral striatum may arise from divergent synaptic effects in these two regions and the different behavioral effects of neuronal connections with these two nuclei. Another important finding from our behavioral studies is the lack of effect of GluD1 ablation from the ventral striatum on social behavior. It has previously been found that glutamatergic projections from the ventral tegmental area to NAc express Cbln1, and are a critical regulator of excitatory neurotransmission and social behavior [25]. Although that study did not probe the postsynaptic partner which may be responsible for these effects, our previous and present results suggest that GluD1 alone may not be responsible for VTA-Cbln1 mediated synaptic and behavioral control of NAc [4]. It is possible that GluD2 may compensate for the loss of GluD1 and serve as postsynaptic Cbln1 partner. It should, however be noted that we did observe social deficit in mice with GluD1 ablation from PV neurons. However, there is a caveat in that, this behavioral deficit may occur either due to the effect of this manipulation in the NAc or elsewhere in the brain. In addition to reduced marble burying and reduced social interaction we also found that ablation of GluD1 from PV neurons produced less mobile events in the forced swim test suggesting less depression-like behavior. Interestingly, motor activity was unaffected in PV-GluD1 KO but MK-801-induced hyperlocomotion was enhanced in PV-GluD1 KO which is relevant to the psychotic phenotype in schizophrenia. Thus, PV-GluD1 KO mice exhibit some features relevant to schizophrenia which is consistent with the association of GRID1 gene that encodes for GluD1 with schizophrenia [36,37]. Overall, it can be concluded from the electrophysiology and local ablation studies that GluD1 plays a critical role in inhibitory neurotransmission in the NAc and regulates behaviors in the anxiety and depression domains.

Supplementary Material

Refer to Web version on PubMed Central for supplementary material.

Funding

This work was supported by grants from the NSF1456818 (SMD), NIH NS104705 (SMD), NIH NS118731 (SMD) and NIH MH116003 (SMD). DC was supported by NIH training grant T32-GM008602.

Data availability

Data is available from the corresponding author upon reasonable request.

References

1. Yuzaki M and Aricescu AR, (2017) A GluD coming-of-age story. Trends Neurosci. 40, 138–150. [PubMed: 28110935]
2. Gupta SC, Yadav R, Pavuluri R, Morley BJ, Stairs DJ and Dravid SM, (2015) Essential role of GluD1 in dendritic spine development and GluN2B to GluN2A NMDAR subunit switch in the cortex and hippocampus reveals ability of GluN2B inhibition in correcting hyperconnectivity. Neuropharmacology. 93, 274–284. [PubMed: 25721396]
3. Liu J, Shelkar GP, Gandhi PJ, Gawande DY, Hoover A, Villalba RM, Pavuluri R, Smith Y and Dravid SM, (2020) Striatal glutamate delta-1 receptor regulates behavioral flexibility and thalamostriatal connectivity. Neurobiol. Dis. 137, 104746. [PubMed: 31945419]
4. Liu J, Gandhi PJ, Pavuluri R, Shelkar GP and Dravid SM, (2018) Glutamate delta-1 receptor regulates cocaine-induced plasticity in the nucleus accumbens. Transl. Psychiatry. 8, 219–018-0273–9. [PubMed: 30315226]
5. Tao W, Diaz-Alonso J, Sheng N and Nicoll RA, (2018) Postsynaptic delta1 glutamate receptor assembles and maintains hippocampal synapses via Cbln2 and neurexin. Proc. Natl. Acad. Sci. U. S. A. 115, E5373–E5381. [PubMed: 29784783]
6. Hepp R, Hay YA, Aguado C, Lujan R, Dauphinot L, Potier MC, Nomura S, Poirel O, El Mestikawy S, Lambolez B and Tricoire L, (2015) Glutamate receptors of the delta family are widely expressed in the adult brain. Brain Struct. Funct. 220, 2797–2815. [PubMed: 25001082]
7. Fossati M, Assendorp N, Gemin O, Colasse S, Dingli F, Arras G, Loew D and Charrier C, (2019) Trans-synaptic signaling through the glutamate receptor delta-1 mediates inhibitory synapse formation in cortical pyramidal neurons. Neuron. 104, 1081–1094.e7. [PubMed: 31704028]
8. Seigneur E and Sudhof TC, (2017) Cerebellins are differentially expressed in selective subsets of neurons throughout the brain. J. Comp. Neurol. 525, 3286–3311. [PubMed: 28714144]
9. Gao J, Maison SF, Wu X, Hirose K, Jones SM, Bayazitov I, Tian Y, Mittleman G, Matthews DB, Zakharenko SS, Liberman MC and Zuo J, (2007) Orphan glutamate receptor delta1 subunit required for high-frequency hearing. Mol. Cell. Biol. 27, 4500–4512. [PubMed: 17438141]
10. Yadav R, Gupta SC, Hillman BG, Bhatt JM, Stairs DJ and Dravid SM, (2012) Deletion of glutamate delta-1 receptor in mouse leads to aberrant emotional and social behaviors. PLoS One. 7, e32969. [PubMed: 22412961]
11. Gupta SC, Ravikrishnan A, Liu J, Mao Z, Pavuluri R, Hillman BG, Gandhi PJ, Stairs DJ, Li M, Ugale RR, Monaghan DT and Dravid SM, (2016) The NMDA receptor GluN2C subunit controls cortical excitatory-inhibitory balance, neuronal oscillations and cognitive function. Sci. Rep. 6, 38321. [PubMed: 27922130]
12. Konno K, Matsuda K, Nakamoto C, Uchigashima M, Miyazaki T, Yamasaki M, Sakimura K, Yuzaki M and Watanabe M, (2014) Enriched expression of GluD1 in higher brain regions and its involvement in parallel fiber-interneuron synapse formation in the cerebellum. J. Neurosci. 34, 7412–7424. [PubMed: 24872547]

13. Raju DV, Shah DJ, Wright TM, Hall RA and Smith Y, (2006) Differential synaptology of vGluT2-containing thalamostriatal afferents between the patch and matrix compartments in rats. J. Comp. Neurol. 499, 231–243. [PubMed: 16977615]

14. Hoover AH, Pavuluri R, Shelkar GP, Dravid SM, Smith Y and Villalba RM, (2021) Ultrastructural localization of glutamate delta 1 (GluD1) receptor immunoreactivity in the mouse and monkey striatum. J. Comp. Neurol. 529, 1703–1718. [PubMed: 33084025]

15. Peters A, Palay SL and Webster H (1991) The Fine Structure of the Nervous System, Oxford University Press, Oxford.

16. Yadav R, Gupta SC, Hillman BG, Bhatt JM, Stairs DJ and Dravid SM, (2012) Deletion of glutamate delta-1 receptor in mouse leads to aberrant emotional and social behaviors. PLoS One. 7, e32969. [PubMed: 22412961]

17. Nicola SM and Malenka RC, (1997) Dopamine depresses excitatory and inhibitory synaptic transmission by distinct mechanisms in the nucleus accumbens. J. Neurosci. 17, 5697–5710. [PubMed: 9221769]

18. Nieto Mendoza E and Hernandez Echeagaray E, (2015) Dopaminergic modulation of striatal inhibitory transmission and long-term plasticity. Neural Plast. 2015, 789502. [PubMed: 26294980]

19. Benamer N, Marti F, Lujan R, Hepp R, Aubier TG, Dupin AAM, Frebourg G, Pons S, Maskos U, Faure P, Hay YA, Lambolez B and Tricoire L, (2018) GluD1, linked to schizophrenia, controls the burst firing of dopamine neurons. Mol. Psychiatry. 23, 691–700. [PubMed: 28696429]

20. Hoffman AF and Lupica CR, (2001) Direct actions of cannabinoids on synaptic transmission in the nucleus accumbens: a comparison with opioids. J. Neurophysiol. 85, 72–83. [PubMed: 11152707]

21. Manzoni OJ and Bockaert J, (2001) Cannabinoids inhibit GABAergic synaptic transmission in mice nucleus accumbens. Eur. J. Pharmacol. 412, R3–5. [PubMed: 11165232]

22. Saunders A, Macosko EZ, Wysoker A, Goldman M, Krienen FM, de Rivera H, Bien E, Baum M, Bortolin L, Wang S, Goeva A, Nemesh J, Kamitaki N, Brumbaugh S, Kulp D and McCarroll SA, (2018) Molecular diversity and specializations among the cells of the adult mouse brain. Cell. 174, 1015–1030.e16. [PubMed: 30096299]

23. Gokce O, Stanley GM, Treutlein B, Neff NF, Camp JG, Malenka RC, Rothwell PE, Fuccillo MV, Sudhof TC and Quake SR, (2016) Cellular taxonomy of the mouse striatum as revealed by single-cell RNA-Seq. Cell. Rep. 16, 1126–1137. [PubMed: 27425622]

24. Qi J, Zhang S, Wang HL, Barker DJ, Miranda-Barrientos J and Morales M, (2016) VTA glutamatergic inputs to nucleus accumbens drive aversion by acting on GABAergic interneurons. Nat. Neurosci. 19, 725–733. [PubMed: 27019014]

25. Krishnan V, Stoppel DC, Nong Y, Johnson MA, Nadler MJ, Ozkaynak E, Teng BL, Nagakura I, Mohammad F, Silva MA, Peterson S, Cruz TJ, Kasper EM, Arnaout R and Anderson MP, (2017) Autism gene Ube3a and seizures impair sociability by repressing VTA Cbln1. Nature. 543, 507–512. [PubMed: 28297715]

26. Uemura T, Lee SJ, Yasumura M, Takeuchi T, Yoshida T, Ra M, Taguchi R, Sakimura K and Mishina M, (2010) Trans-synaptic interaction of GluRdelta2 and Neurexin through Cbln1 mediates synapse formation in the cerebellum. Cell. 141, 1068–1079. [PubMed: 20537373]

27. Matsuda K, Miura E, Miyazaki T, Kakegawa W, Emi K, Narumi S, Fukazawa Y, Ito-Ishida A, Kondo T, Shigemoto R, Watanabe M and Yuzaki M, (2010) Cbln1 is a ligand for an orphan glutamate receptor delta2, a bidirectional synapse organizer. Science. 328, 363–368. [PubMed: 20395510]

28. Yuzaki M, (2018) Two classes of secreted synaptic organizers in the central nervous system. Annu. Rev. Physiol. 80, 243–262. [PubMed: 29166241]

29. Ryu K, Yokoyama M, Yamashita M and Hirano T, (2012) Induction of excitatory and inhibitory presynaptic differentiation by GluD1. Biochem. Biophys. Res. Commun. 417, 157–161. [PubMed: 22138648]

30. Yadav R, Hillman BG, Gupta SC, Suryavanshi P, Bhatt JM, Pavuluri R, Stairs DJ and Dravid SM, (2013) Deletion of glutamate delta-1 receptor in mouse leads to enhanced working memory and deficit in fear conditioning. PLoS One. 8, e60785. [PubMed: 23560106]

31. Miura E, Iijima T, Yuzaki M and Watanabe M, (2006) Distinct expression of Cbln family mRNAs in developing and adult mouse brains. Eur. J. Neurosci. 24, 750–760. [PubMed: 16930405]

32. Paul EJ, Tossell K and Ungless MA, (2019) Transcriptional profiling aligned with in situ expression image analysis reveals mosaically expressed molecular markers for GABA neuron sub-groups in the ventral tegmental area. Eur. J. Neurosci. 50, 3732–3749. [PubMed: 31374129]

33. Treit D, Pinel JP and Fibiger HC, (1981) Conditioned defensive burying: a new paradigm for the study of anxiolytic agents. Pharmacol. Biochem. Behav. 15, 619–626. [PubMed: 6117086]

34. De Boer SF and Koolhaas JM, (2003) Defensive burying in rodents: ethology, neurobiology and psychopharmacology. Eur. J. Pharmacol. 463, 145–161. [PubMed: 12600707]

35. Thomas A, Burant A, Bui N, Graham D, Yuva-Paylor LA and Paylor R, (2009) Marble burying reflects a repetitive and perseverative behavior more than novelty-induced anxiety. Psychopharmacology (Berl). 204, 361–373. [PubMed: 19189082]

36. Fallin MD, Lasseter VK, Avramopoulos D, Nicodemus KK, Wolyniec PS, McGrath JA, Steel G, Nestadt G, Liang KY, Huganir RL, Valle D and Pulver AE, (2005) Bipolar I disorder and schizophrenia: a 440-single-nucleotide polymorphism screen of 64 candidate genes among Ashkenazi Jewish case-parent trios. Am. J. Hum. Genet. 77, 918–936. [PubMed: 16380905]

37. Guo SZ, Huang K, Shi YY, Tang W, Zhou J, Feng GY, Zhu SM, Liu HJ, Chen Y, Sun XD and He L, (2007) A case-control association study between the GRID1 gene and schizophrenia in the Chinese Northern Han population. Schizophr. Res. 93, 385–390. [PubMed: 17490860]

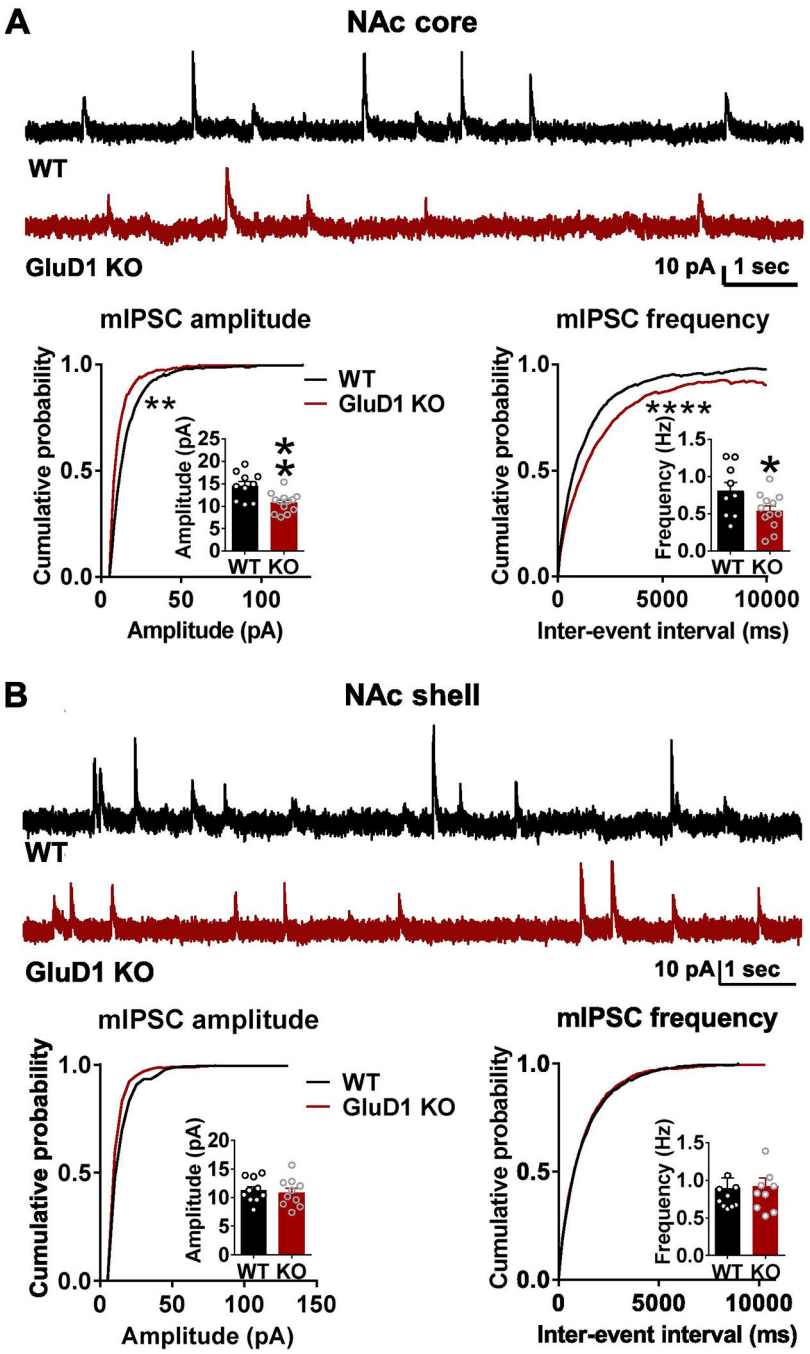

Fig. 1.

Loss of GluD1 reduces mIPSC amplitude and frequency in the NAc core but not shell. **A**. A significant reduction in the amplitude of mIPSC was observed in MSNs from NAc core of GluD1 KO (WT: 14.55 ± 0.9841 pA vs. GluD1 KO: 10.82 ± 0.6042 pA, $p = 0.0028$, Unpaired t-test). Inter-event interval (IEI) was also significantly reduced ($p = 0.0096$, K-S test) (N = 10–13 from 3 to 4 animals per genotype). A significant reduction in frequency of mIPSC was also observed in GluD1 KO (WT: 0.8073 ± 0.1159 Hz vs. St-GluD1 KO: 0.5390 ± 0.06883 Hz, $p = 0.0491$, Unpaired t-test). Inter-event interval (IEI) was also significantly

reduced ($p = 0.0001$, K-S test). **B**. No significant change in mIPSC amplitude or frequency was observed in NAc shell (amplitude: WT: 11.26 ± 0.6671 pA vs. GluD1 KO: 10.87 ± 0.7836 pA, $p = 0.7087$; frequency: WT: 0.8968 ± 0.1323 Hz vs. GluD1 KO: 0.9187 ± 0.1054 Hz, $p = 0.8984$; Unpaired t-test) (N = 10 from 3 to 4 animals per genotype). All data are presented as mean ± SEM

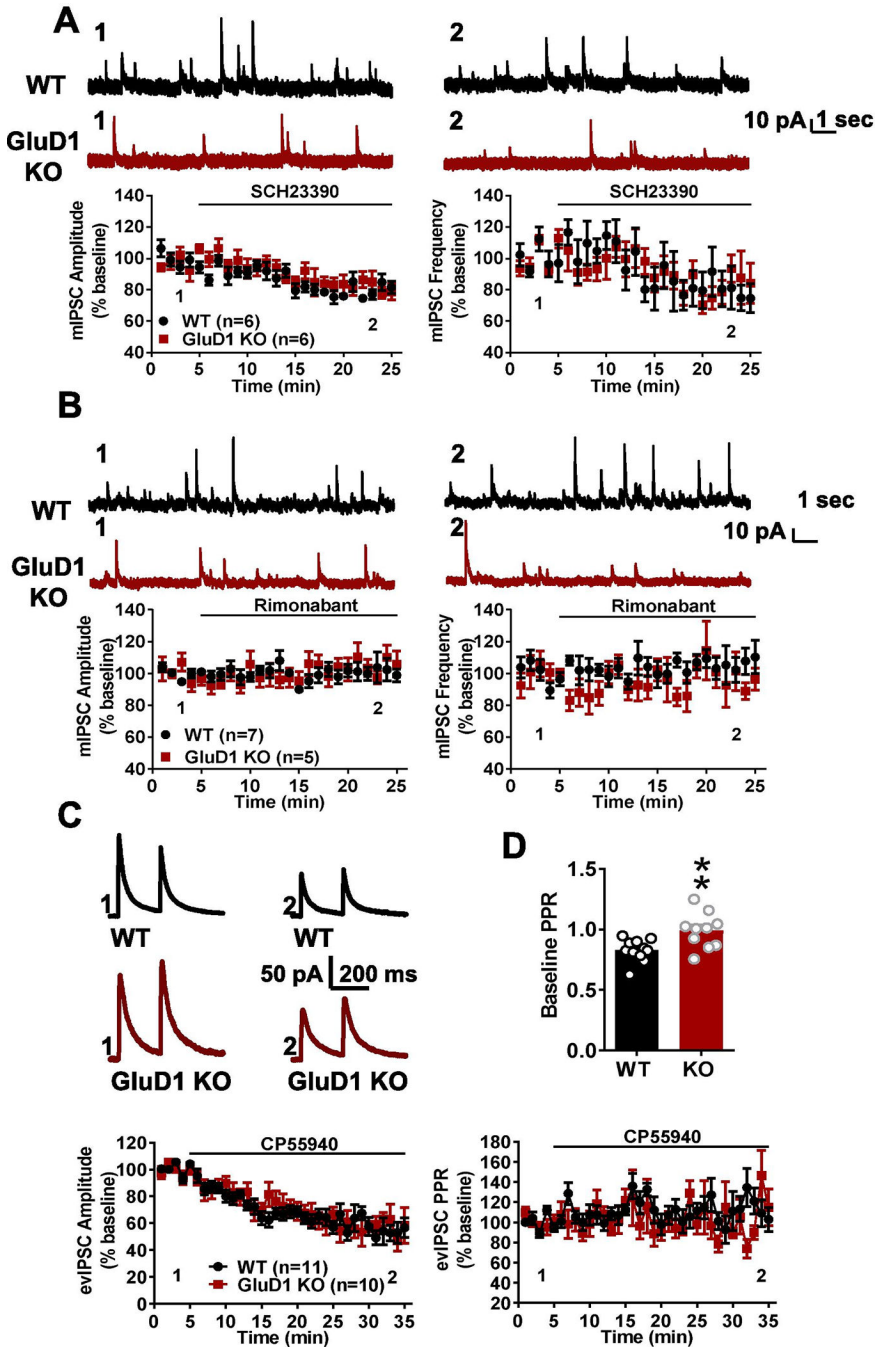

Fig 2.

No change in basal dopamine and cannabinoid tone or inhibitory plasticity in MSNs in NAc core but change in inhibitory transmitter release probability. **A**. Application of D1 receptor antagonist SCH23390 (10 μM) reduced the amplitude and frequency of mIPSC from MSNs in NAc core. Similar extent of reduction in mIPSC characteristics were observed in both wildtype and GluD1 KO (N = 6 from 3 animals per genotype). **B**. CB1 receptor inverse agonist (rimonabant) did not affect mIPSCs in both wildtype and GluD1 KO suggesting no change in basal endocannabinoid tone (N = 5–7 from 3 animals per genotype). **C**. Evoked

paired-pulse IPSC responses were obtained from MSNs in NAc core. Application of CB1 agonist CP55940 (2 μM) reduced the evoked IPSC response in both wildtype and GluD1 KO MSNs to similar extent (N = 10–11 from 3 animals per genotype). **D**. Significantly higher baseline paired-pulse ratio of the IPSC was observed in GluD1 KO (WT: 0.8284 ± 0.02757 vs. GluD1 KO: 0.9891 ± 0.04632, $p = 0.0066$; Unpaired t-test)

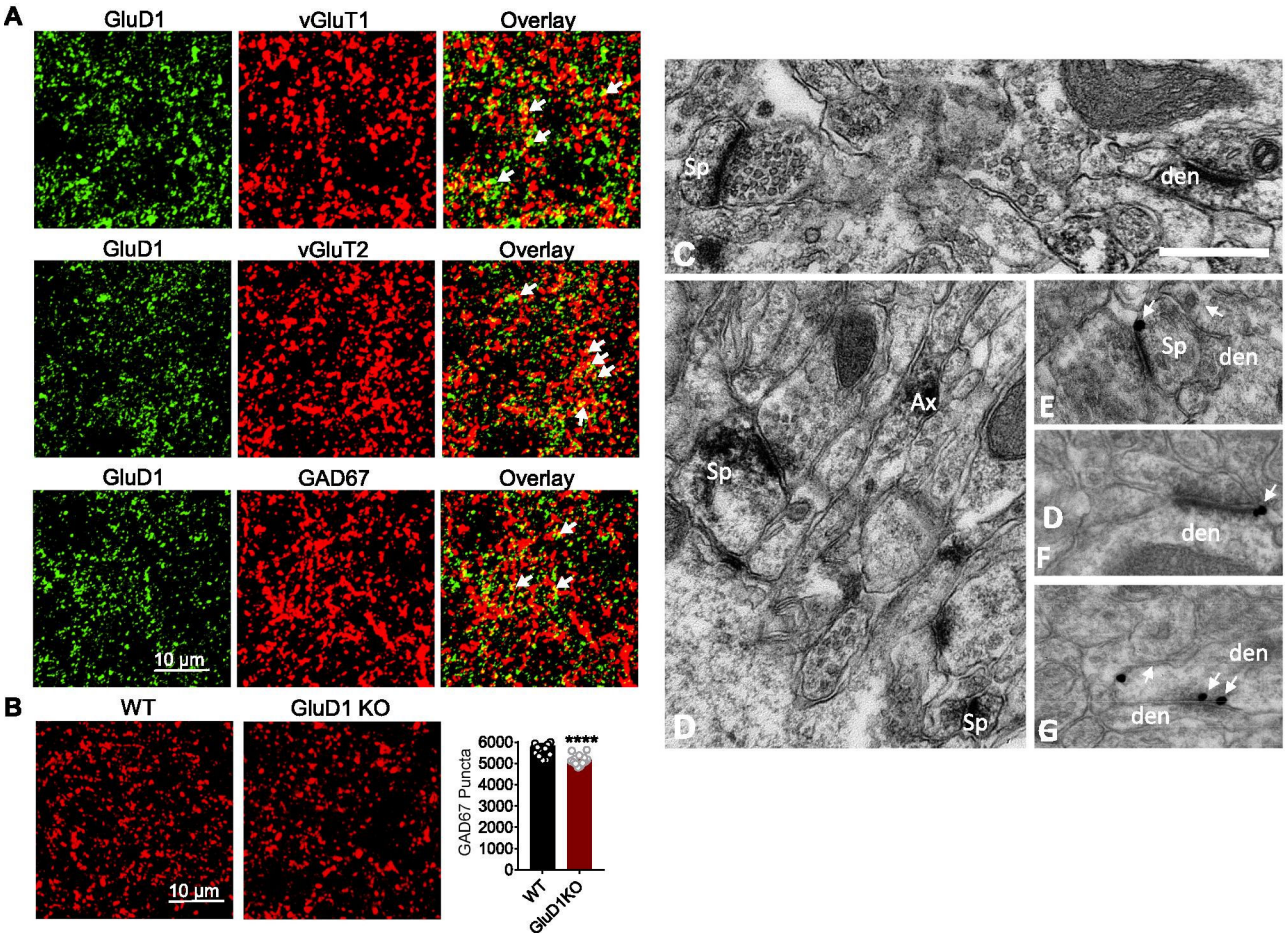

Fig. 3.

GluD1 is localized to both excitatory and inhibitory synapses in the NAc core and loss of GluD1 reduces inhibitory synaptic puncta. **A**. Representative confocal images from NAc core of GluD1 WT mice showing colocalization of GluD1 with excitatory markers vGluT1 and vGluT2. GluD1 also colocalized with inhibitory marker GAD67. **B**. Representative coronal images passing through NAc core of WT and GluD1 KO mice immunolabelled for GAD67. Quantification of immunostaining showed significant reduction in GAD67 puncta in GluD1 KO in the NAc core ($p < 0.0001$; Unpaired t-test). **C**–**G**. Electron micrographs of GluD1-immunoreactive profiles in the mouse nucleus accumbens core. (**C**–**D**) Examples of GluD1-immunoreactive spine (Sp), dendritic (den) and axonal (Ax) profiles localized with immunoperoxidase, (**E**–**F**) GluD1 immunogold labeling (arrows) perisynaptic to asymmetric axo-spinous (**E**) and axo-dendritic (**F**) synapses, (**G**) GluD1 immunogold labeling in the main body of a symmetric axo-dendritic synapse (double arrows). Scale bar: 0.5 µm (valid for A–E)

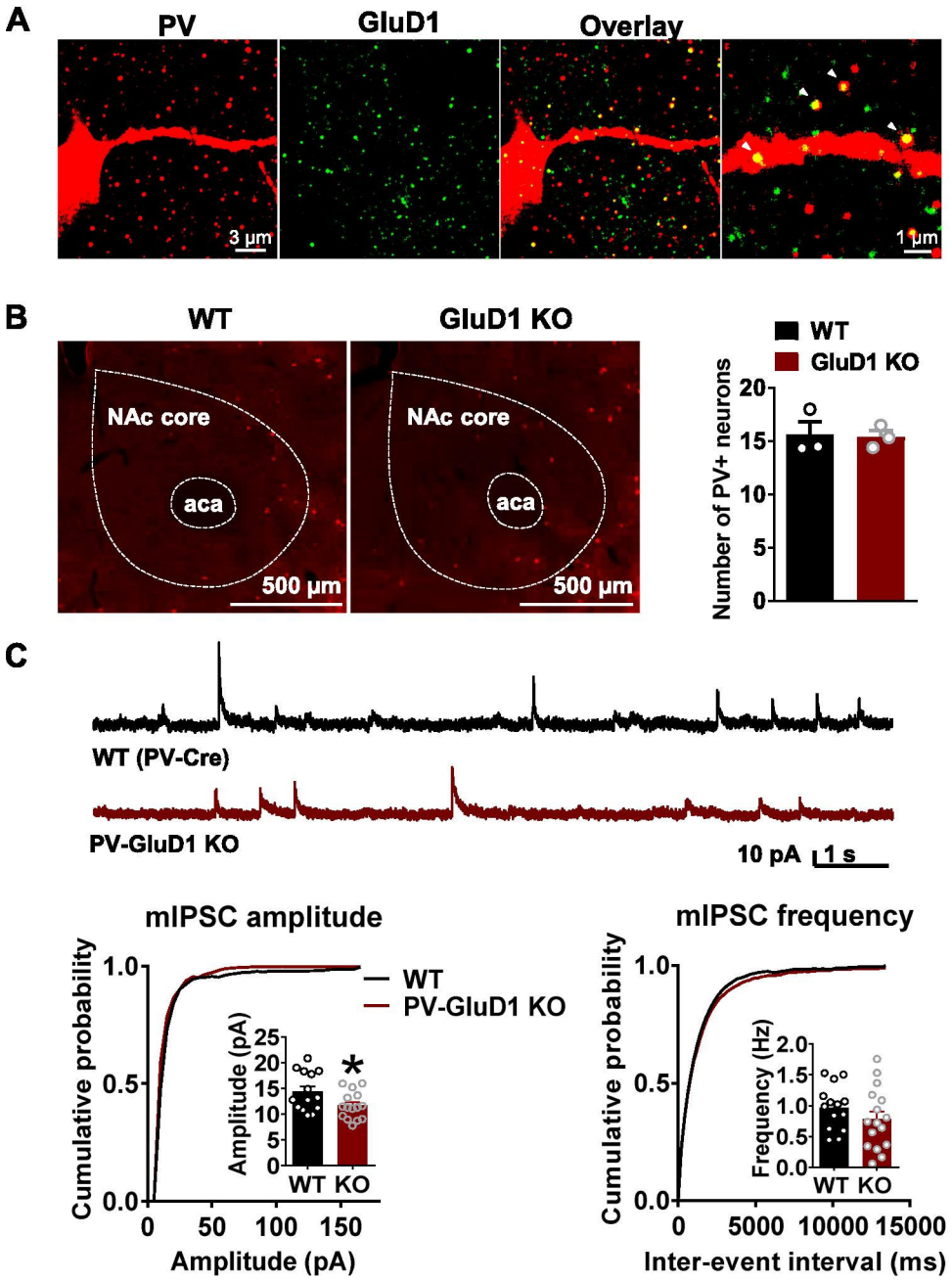

Fig. 4.

GluD1 ablation from PV neurons reduces the inhibitory neurotransmission in the NAc core. **A**. GluD1 was found to colocalize to PV neurons in the NAc core. Immunohistochemical analysis for GluD1 (green) and PV (red) indicates that GluD1 localizes on dendrites and soma of PV neurons in the NAc core. **B**. No change in the number of PV neurons in the NAc upon ablation of GluD1 from PV neurons (N = 3 per genotype). **C**. Modest reduction in the amplitude of mIPSC but no change in frequency in mice with GluD1 ablation from PV neurons. Reduction in the amplitude of mIPSCs in PV-GluD1 KO (WT: 14.38 ± 1.012 pA

vs. PV-GluD1 KO: 11.68 ± 0.6857 pA, $p = 0.0337$, Unpaired t-test; N = 14–15 from 3 to 4 animals per genotype)

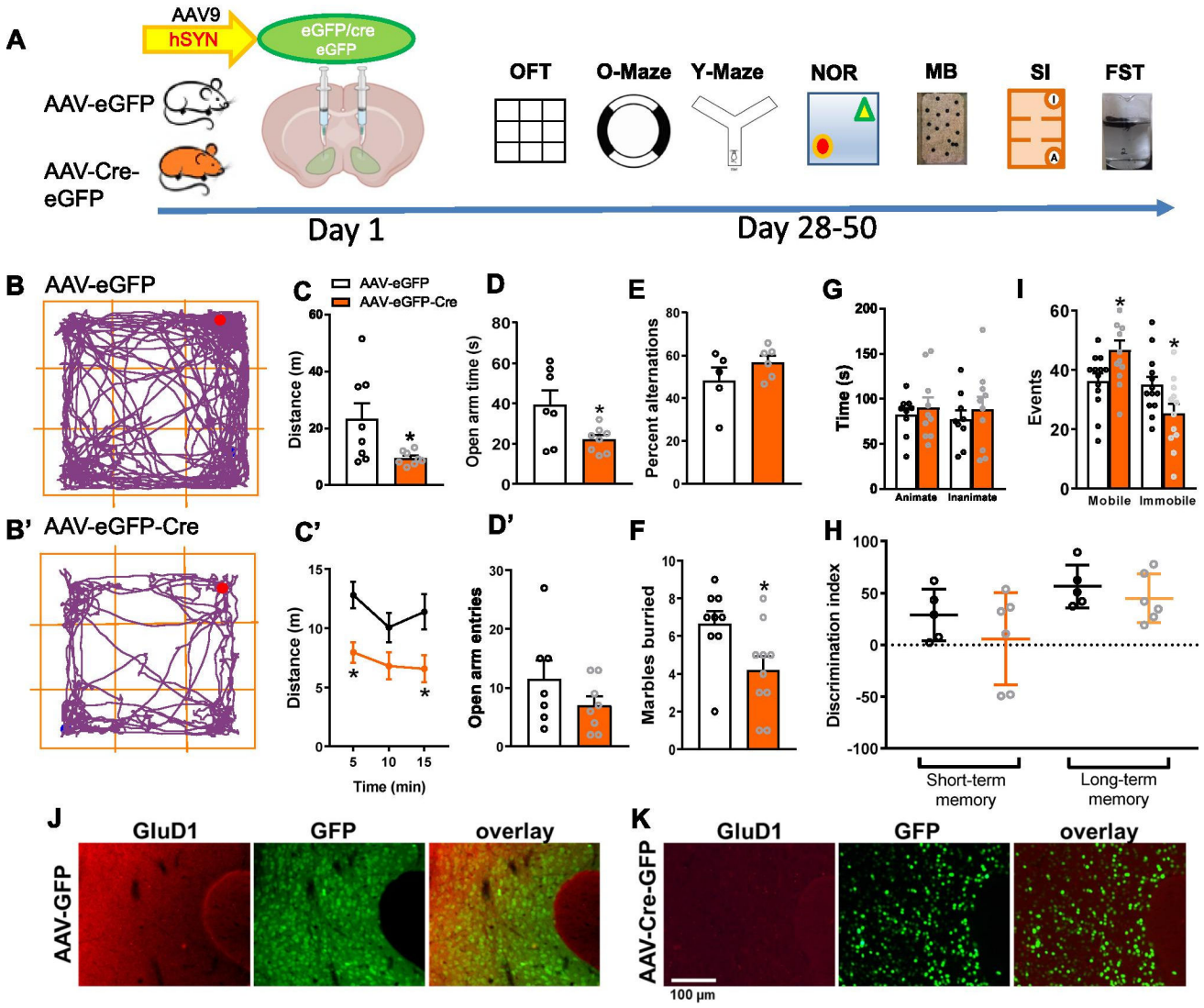

Fig. 5.

Selective ablation of GluD1 from the NAc leads to hypolocomotion and affects anxiety- and depression-like behaviors. **A**. Experimental timeline, GluD1$^{flox/flox}$ mice received bilateral micro injections of AAV-eGFP and AAV-eGFP-Cre (Day 1) into the ventral striatum (VS), followed by behavioral assays (Day 28–50). **B** and **B'**. Representative track plots of the path travelled by mice (VS-AAV-eGFP and VS-AAV-eGFP-Cre). **C**. VS-AAV-eGFP-Cre group showed significantly less distance traveled compared to the VS-AAV-eGFP group (VS-AAV-eGFP 23.25 ± 5.522 (N = 8) vs VS-AAV-eGFP-Cre 9.532 ± 0.8487 (N = 8), p = 0.0423, unpaired t-test). **C'**. Locomotor activity per 5 min revealed a significant effect of GluD1 deletion ([F (1, 45)=20.17, $p < 0.0001$], Two-way ANOVA, Bonferroni's post-hoc test, $p < 0.05$). **D** and **D'**. VS-AAV-eGFP-Cre group showed significantly less time spent in open arm in zero maze (VS-AAV-eGFP 39.29 ± 6.972 (N = 7) vs VS-AAV-eGFP-Cre 21.95 ± 2.204 (N = 8), p = 0.0486) compared to the VS-AAV-eGFP group but no change in number of entries (VS-AAV-eGFP 11.57 ± 3.108 vs. VS-AAV-eGFP-Cre 7 ± 1.558, p = 0.2214, unpaired t-test). **E**. No change in percent alternations in Y-maze test (N = 5–6,

$p = 0.2194$, unpaired t-test). **F**. In marble burying test, VS-AAV-eGFP-Cre group buried significantly fewer marbles compared to the VS-AAV-eGFP group (VS-AAV-eGFP 6.667 ± 0.667 (N = 9) vs. VS-AAV-eGFP-Cre 4.2 ± 0.7272 (N = 10), $p = 0.0229$, unpaired t-test). **G**. In the sociability test no significant difference in time interacting with the stranger mouse (animate) (N = 9–10, $p = 0.5726$, unpaired t-test) and inanimate chamber was observed ($p = 0.5365$, unpaired t-test). **H**. In novel object recognition test no change in short-term (N = 5–6, $p = 0.3133$, unpaired t-test) and long-term ($p = 0.4098$, unpaired t-test) memory was observed. **I**. In a forced swim test VS-AAV-eGFP-Cre group showed significantly more mobility events (VS-AAV-eGFP 36.23 ± 2.61 (N = 13) vs. VS-AAV-eGFP-Cre 46.58 ± 3.408 (N = 12), $p = 0.0251$, unpaired t-test) and significantly less immobility events (VS-AAV-eGFP 34.92 ± 2.781 vs. VS-AAV-eGFP-Cre 25.25 ± 3.36, $p = 0.0373$, unpaired t-test) compared to VS-AAV-eGFP mice. All data are presented as mean ± SEM. **J**. AAV-eGFP expression and GluD1 expression level was evaluated after the completion of behavioral experiments using immunohistochemical analysis. Sections from brain were evaluated for AAV-eGFP expression (green) and immunohistochemistry was performed for GluD1 (red). **K**. Downregulation of GluD1 (red) was observed in AAV-eGFP-Cre (green) injected animals

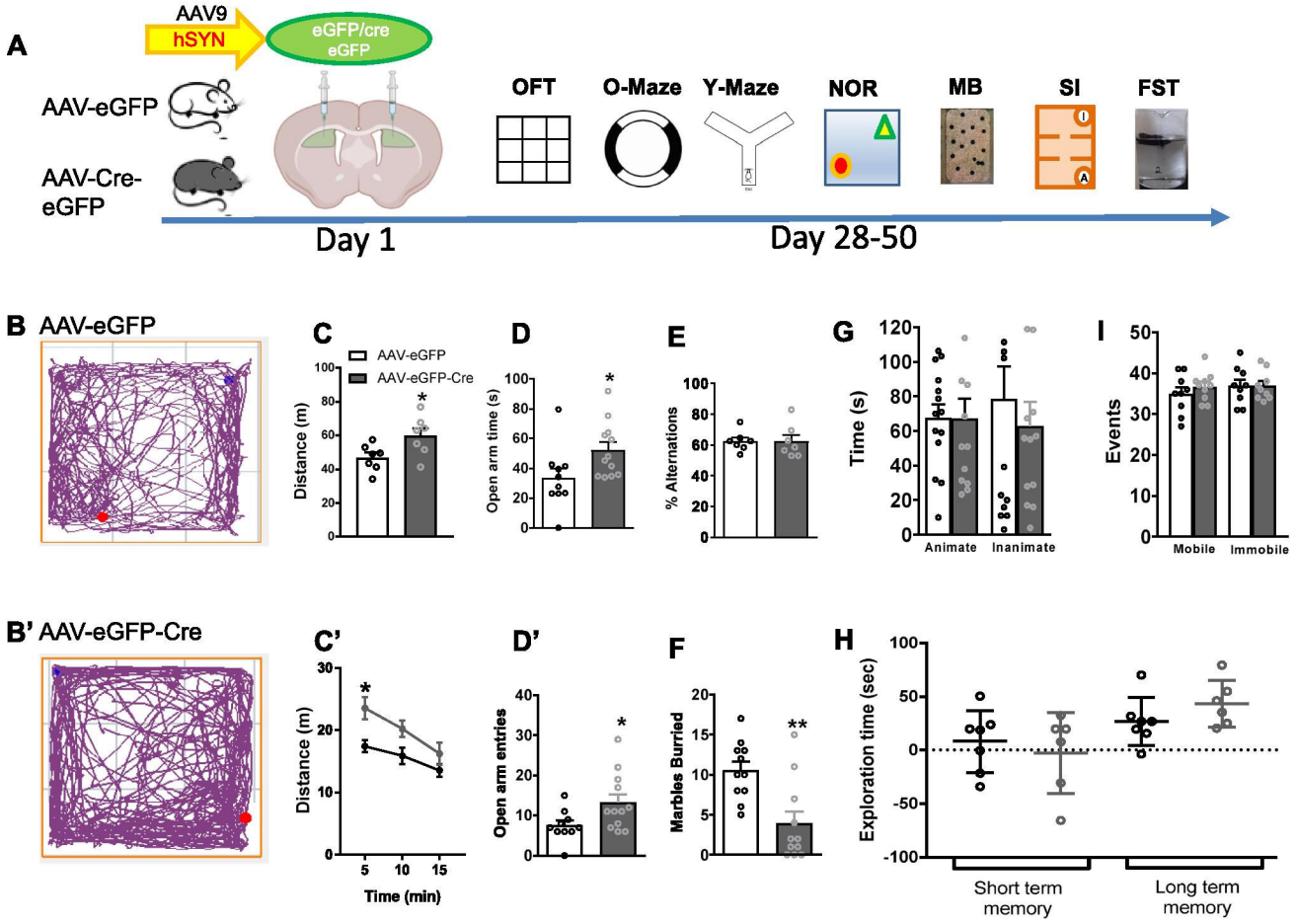

Fig. 6.

Effect of GluD1 ablation from dorsal striatum on behavior. **A**. Experimental timeline, GluD1$^{flox/flox}$ mice received bilateral micro injections of AAV-eGFP and AAV-eGFP-Cre (Day 1) into the dorsal striatum (DS), followed by behavioral assays (Day 28–50). **B** and **B'**. Representative track plots of the path travelled by mice (DS-AAV-eGFP and DS-AAV-eGFP-Cre). **C**. DS-AAV-eGFP-Cre group showed significantly more distance traveled compared to the DS-AAV-eGFP group (DS-AAV-eGFP 46.83 ± 2.954 (N = 7) vs. DS-AAV-eGFP-Cre 59.98 ± 4.406 (N = 7), $p = 0.0316$, unpaired t-test). **C'**. Locomotor activity per 5 min revealed a significant effect of GluD1 deletion ([F (1, 12)=6.143, $p = 0.0290$], Two-way ANOVA, Bonferroni's post-hoc test, $p = 0.0111$). **D** and **D'**. DS-AAV-eGFP-Cre group showed significantly more time spent in open arm of zero maze (DS-AAV-eGFP 33.45 ± 6.487 (N = 10) vs. DS-AAV-eGFP-Cre 52.25 ± 5.365 (N = 12), $p = 0.0382$, unpaired t-test) and more number of entries (DS-AAV-eGFP 7.5 ± 1.222 vs DS-AAV-eGFP-Cre 13.25 ± 2.06, $p = 0.0278$, unpaired t-test). **E**. No change in percent alternation in the Y-maze test (N = 7, $p > 0.9999$, unpaired t-test). **F**. In marble burying test, DS-AAV-eGFP-Cre group buried significantly fewer marbles (DS-AAV-eGFP 10.55 ± 1.098 (N = 11) vs. DS-AAV-eGFP-Cre 3.909 ± 1.516 (N = 11), $p = 0.0020$, unpaired t-test). **G**. In the sociability test no significant difference in time interacting with the stranger mouse (animate) (N = 13–14, $p = 0.9813$, unpaired t-test) and inanimate chamber ($p = 0.5120$, unpaired t-test). **H**. In novel object

recognition test no change in short-term (N = 6– 7, $p = 0.5672$, unpaired t-test) or long-term memory ($p = 0.1982$, unpaired t-test). **I**. In a forced swim test no significant difference in mobility events (N = 9–10, $p = 0.3651$, unpaired t-test) and immobility events ($p > 0.9999$, unpaired t-test). All data are presented as mean ± SEM

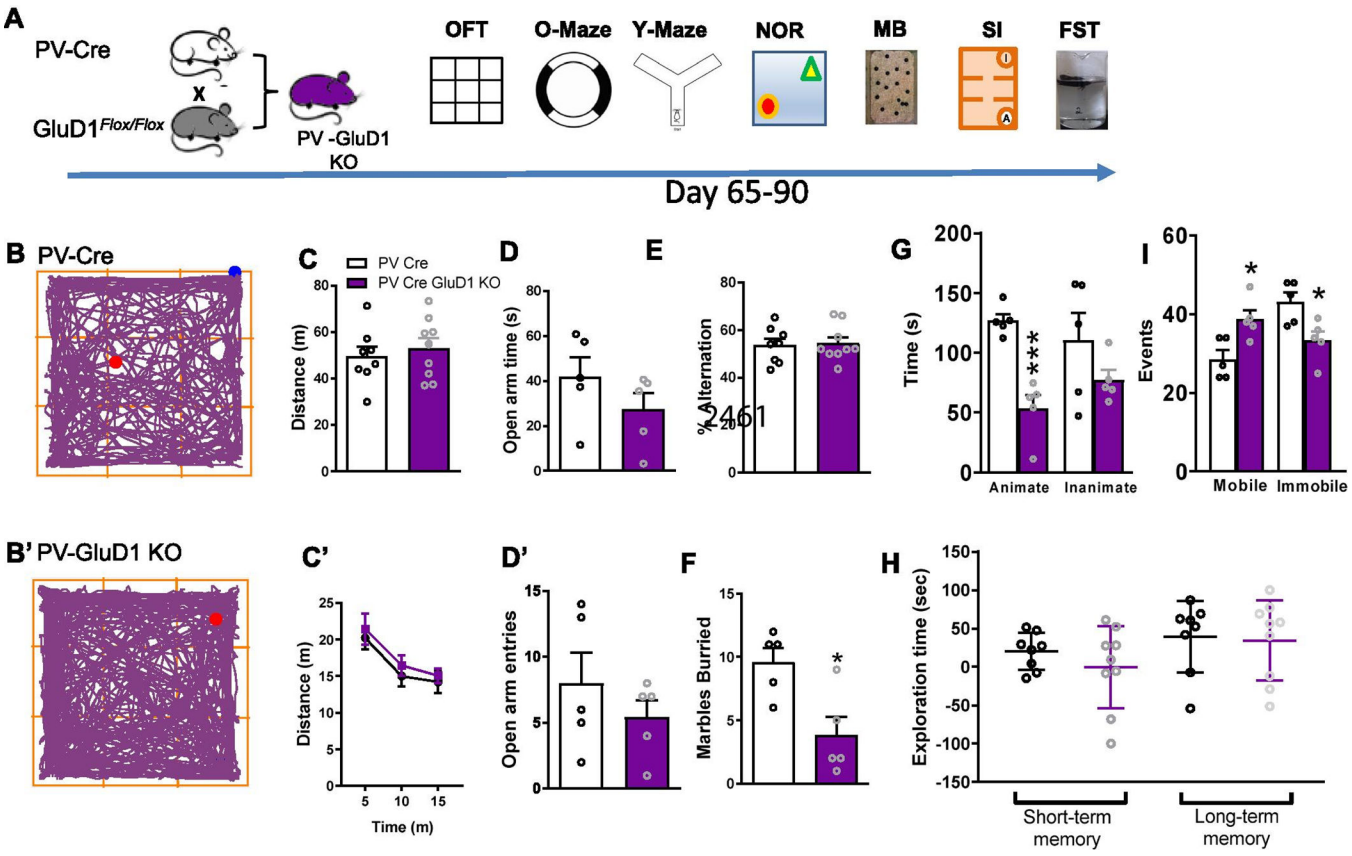

Fig. 7.

Effect of GluD1 ablation from PV neurons on anxiety- and depression-like behavior. **A**. Breeding strategy and experimental timeline, GluD1$^{flox/flox}$ mice were crossed with the PV-Cre mice to produce PV-GluD1 KO. Behavioral experiments were conducted on Day 65–90. **B** and **B'**. Representative track plots of the path travelled by mice (PV-Cre and PV-GluD1 KO). **C**. PV-GluD1 KO mice did not show any significant change in distance traveled compared to the PV-Cre mice (N = 8–9, $p = 0.5633$, unpaired t-test). **C'**. Further the locomotor activity per 5 min was also similar between groups. **D** and **D'**. No change in time spent in open arm (N = 5, $p = 0.2387$, unpaired t-test) or number of entries ($p = 0.3597$, unpaired t-test). **E**. No change in percent alternation in Y-maze test (N = 8–9, $p = 0.8400$, unpaired t-test). **F**. In marble burying test, PV-GluD1 KO mice buried significantly fewer marbles compared to the PV-Cre mice (PV-Cre 9.6 ± 1.122 (N = 5) vs. PV-GluD1 KO 3.8 ± 1.463 (N = 5), $p = 0.0137$, unpaired t-test). **G**. In the sociability test, PV-GluD1 KO mice showed significantly less interaction time with the stranger mouse (animate) (PV Cre 126.9 ± 5.582 (N = 5) vs. PV-GluD1 KO 53.58 ± 11.11 (N = 5), $p = 0.0004$, unpaired t-test) compared to the PV-Cre mice. No difference in inanimate chamber exploration between groups ($p = 0.2072$, unpaired t-test). **H**. In novel object recognition test no change in short-term (N = 8–9, $p = 0.3363$, unpaired t-test) or long-term memory ($p = 0.8506$, unpaired t-test). **I**. In a forced swim test PV-GluD1 KO mice showed significantly more mobility events (PV-Cre 28.6 ± 2.272 (N = 5) vs. PV-GluD1 KO 38.8 ± 2.289 (N = 5), $p = 0.0133$, unpaired t-test) and less immobility events (PV-Cre 43.2 ± 2.396 vs. PV-GluD1 KO 33.4 ±

2.337 $p = 0.0190$, unpaired t-test) compared to PV-Cre mice. All data are presented as mean ± SEM